

Inspiral of Generic Black Hole Binaries: Spin, Precession, and Eccentricity

Janna Levin^{1,2}, Sean T. McWilliams^{1,2,3}, and Hugo Contreras⁴

¹*Department of Physics and Astronomy,
Barnard College of Columbia University,
3009 Broadway, New York, NY 10027*

²*Institute for Strings, Cosmology and Astroparticle Physics (ISCAP),
Columbia University, New York, NY 10027*

³*Department of Physics, Princeton University, Princeton, NJ 08544 and*

⁴*Department of Physics, Columbia University, New York, NY 10027**

Given the absence of observations of black hole binaries, it is critical that the full range of accessible parameter space be explored in anticipation of future observation with gravitational wave detectors. To this end, we compile the Hamiltonian equations of motion describing the conservative dynamics of the most general black hole binaries and incorporate an effective treatment of dissipation through gravitational radiation, as computed by Will and collaborators. We evolve these equations for systems with orbital eccentricity and precessing spins. We find that, while spin-spin coupling corrections can destroy constant radius orbits in principle, the effect is so small that orbits will reliably tend to quasi-spherical orbits as angular momentum and energy are lost to gravitational radiation. Still, binaries that are initially highly eccentric may retain eccentricity as they pass into the detectable bandwidth of ground-based gravitational wave detectors. We also show that a useful set of natural frequencies for an orbit demonstrating both spin precession and periastron precession is comprised of (1) the frequency of angular motion in the orbital plane, (2) the frequency of the plane precession, and (3) the frequency of radial oscillations. These three natural harmonics shape the observed waveform.

*Electronic address: janna@astro.columbia.edu

I. INTRODUCTION

Motivated by future gravitational-wave observatories, a campaign to track the inspiral of the most generic black hole binaries has long been underway [1–11]. The promise of gravitational-wave astronomy lies in our ability to observe and test the full range of astrophysical phenomena, including spinning, precessing, eccentric pairs of unequal mass. To this end, Will and collaborators have published a series of computations of the equations governing black hole binary motion in the Post-Newtonian (PN) expansion to 3.5PN order, including spin corrections [8–11]. We compile those results in an appendix to provide a resource for probing and testing the PN dynamics. We then convert the dissipative terms into Hamiltonian variables and suggest a modification of the Hamiltonian equations of motion that incorporates the effects of radiation reaction. The modified Hamiltonian formulation and the Lagrangian formulation admit equivalent descriptions, though for the purposes of investigating the natural harmonics of these systems we will exploit the ease of interpretation offered by the Hamiltonian formulation.

Binary stars that evolve to a pair of black holes can show evidence of eccentricity and spin precession in waveforms detectable by LISA [12]. Although long-lived pairs will likely shed eccentricity by the time they enter the LIGO bandwidth, the entire orbital plane continues to precess along with the spins. Also, black hole pairs formed by tidal capture in globular clusters or galactic nuclei may retain significant eccentricity as their signals pass through the band of current and future ground-based gravitational-wave observatories [13, 14]. The equations of motion of Refs. [8–11] allow flexibility in handling the gravitational radiation emitted by any realistic black hole pair, prior to entering the strong-field.

There are four questions we can address immediately with this compilation of the inspiral equations: (1) Do spinning pairs tend to quasi-spherical orbits? (2) What features are generically introduced into waveforms through periastron precession and spin precession? (3) How much energy is lost during each burst near periastron passage? (4) How much of the orbit and the waveform for eccentric, precessing orbits is well-described by the PN expansion?

The first question (Do spinning pairs tend to quasi-spherical orbits?) must be asked since the purely circular orbits are destroyed by spin-spin (SS) couplings. When spin-orbit (SO) coupling is incorporated, the entire orbital-plane precesses and the quasi-circular orbits are

replaced by quasi-spherical orbits – trajectories that lie on the surface of a sphere whose radius shrinks only due to dissipation. However, spin-spin couplings actually destroy even these so that there are no constant radius orbits, even if we were to artificially turn off dissipation by turning off the half-order terms in the expansion. In other words, if black holes spin, *there may not be any quasi-spherical* orbits and all orbits could retain eccentricity at all stages of their inspiral. We can ask how significant the effect is. Since spin-spin is a subdominant effect, we find that the eccentric behavior is small and that orbits can appear to be very nearly quasi-spherical.

The second question (What features are generically introduced into waveforms through periastron precession and spin precession?) is significant for designing optimal detection algorithms and estimating source parameters. For systems possessing spin, modulation due to orbital plane precession will leave an imprint on the observed waveform. In the case of significant eccentricity, the waveforms are modulated by the radial oscillation of the orbit. Characteristically the amplitude is modulated by eccentricity, as is the polarization due to the precession of the periastron and the orbital plane. The Fourier transform of the waveform will reflect these precessions by reflecting the natural frequencies of the orbit, which modulate the frequency evolution from loss of orbital energy that is present in all black hole binaries. We demonstrate these features for an example black hole binary that possesses all three characteristic frequencies, for which we also address the third question posed (How much energy is lost during each burst near periastron passage?).

The fourth question (How much of the orbit and waveform for eccentric, precessing orbits is well described by the PN expansion?) has not been addressed for generic orbits. In the limit of quasi-spherical orbits, the dynamics and waveform are usually taken to be accurate until the system reaches the innermost stable circular orbit (ISCO), beyond which even the conservative dynamics cannot be treated adiabatically. However, the ISCO is formally a characteristic of a test-particle orbit in Schwarzschild or Kerr spacetime, and is not well defined for binary spacetimes. As we will show, the PN sequence actually diverges well outside the ISCO not only for eccentric precessing systems, but for quasi-spherical systems as well. We find that the breakdown happens at radial separations $r \sim 10M$, which is well outside the Schwarzschild ISCO ($6M$), in contrast to the conventional wisdom of using $6M$ as a reference point for truncating PN approximations.

Due to this limitation of the approximation, the PN equations of motion cannot be used

to probe the most extreme form of precession manifest as zoom-whirl behavior – elliptical zooms out to apastron followed by multiple nearly circular whirls around periastron [15]. Zoom-whirl orbits are most prevalent when periastron drops into the strong-field regime. As shown in Ref. [16], complete whirls occur when periastron falls between the IBCO (innermost bound circular orbit) and the ISCO. To be clear, zoom-whirl orbits exist and have been observed in numerical relativity simulations [17, 18]; they are simply beyond the trusted regime for the PN approximation.

To lay the foundation, we begin with a discussion of conservative black hole dynamics in §II. In §III, we discuss the utility of a Hamiltonian formulation of the equations of motion for simplifying interpretation of the dynamics of the full inspiral trajectories and resulting gravitational waveforms for spinning black hole pairs on eccentric, precessing orbits. In §IV, we explore the limits of our, and indeed any, PN formulation, due to the intrinsic non-perturbative nature of the dynamics at the end of the inspiral. In §V, we summarize the results and the answers to the four questions we posed. For completeness and ease of reference, in §A the PN corrections to the equations of motion including the dissipation due to gravitational radiation are compiled from Refs. [8–11] as derived by Will and collaborators to 3.5PN order with SO and SS coupling. Finally, in §B, we convert the PN corrections originally computed in the Lagrangian formulation into Hamiltonian coordinates, which is the approach we apply throughout the text.

II. DYNAMICS WITHOUT DISSIPATION

For this section, radiation reaction has artificially been turned off so the pair shows no evidence of dissipation. The advantage of doing so is that we can clearly see intrinsic features of the dynamics that dissipation can obscure. In the following section, dissipation is included while the insights of this section will continue to guide our perspective.

If either of the black holes spin, orbital motion famously no longer lies in a plane in the absence of special symmetries. The black holes engage in an intricate three-dimensional motion tangled by precession. An example of the three-dimensional range of a spinning pair is shown in center-of-mass coordinates on the far left of Fig. 1. We want to highlight the two different precession effects: periastron precession and precession of the orbital plane. The two effects can be cleanly separated with a natural choice of coordinates [19, 20].

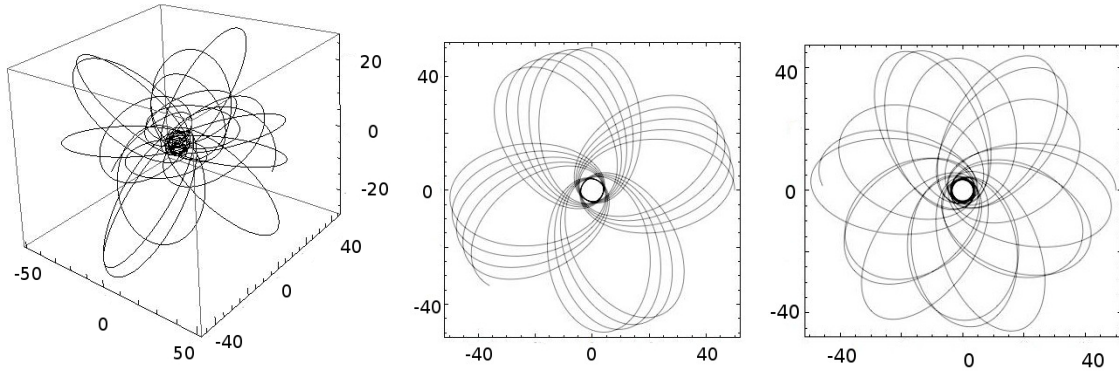


FIG. 1: A black hole pair with $m_2/m_1 = 1/4$. The heavier of the two black holes is spinning at 0.9 maximal. The lighter is not spinning. Left: The orbit. Middle: The orbit in the orbital plane showing the constancy of the periastron and apastron as well as isolating the periastron precession. In the orbital plane, the pair precesses around a four-leaf clover. Right: A projection of the orbit onto the equatorial plane, showing that the innate symmetry of the orbit is obscured.

First, consider precession of the orbital plane. If the spins of the black hole and the orbital angular momentum are aligned or anti-aligned, motion will lie in the equatorial plane, defined as the plane perpendicular to the total angular momentum, $\mathbf{J} = \mathbf{L} + \mathbf{S}$, where \mathbf{L} is the orbital angular momentum and \mathbf{S} is the sum of the spins. However, when the spins are not aligned with the orbital angular momentum, the spins will precess around the total angular momentum, and by conservation of the total momentum (i. e. $\dot{\mathbf{J}} = 0$), the orbital angular momentum will precess to compensate (i. e. $\dot{\mathbf{L}} = -\dot{\mathbf{S}}$). Since the orbital plane is spanned by (\mathbf{r}, \mathbf{p}) and is orthogonal to the orbital angular momentum, $\mathbf{L} = \mathbf{r} \times \mathbf{p}$, as shown in Fig. 2, the entire orbital plane precesses. Plane precession is a purely relativistic reflection of black hole spins and so isolating the effect draws out distinct signatures for parameter estimation.

Periastron precession can be isolated, in turn, by following the motion confined to the orbital plane. In Ref. [19, 20], it was shown that when there is one effective spin – defined by one black hole spinning or two equal-mass black holes with arbitrary spins – that periastron and apastron are constants and the periastron precesses at a fixed rate, as shown in the middle panel of 1. By contrast, these precise features are obscured in the equatorial plane, as shown by the projection in the far right panel of 1. So, to separate periastron precession from the precession of the orbital plane, we select a coordinate system that cleaves the two effects.

The coordinate system that affects this separation is given by (r, Φ, Ψ) where r is the radial coordinate, Φ is the angle swept out in the orbital plane, and Ψ is the angle swept out as \mathbf{L} swings around \mathbf{J} [19, 20]. The polar coordinates in the orbital plane that precess through space as the plane precesses are $(\hat{\mathbf{n}}, \hat{\Phi})$ with

$$\hat{\Phi} = \hat{\mathbf{L}} \times \hat{\mathbf{n}} \quad . \quad (1)$$

where $\hat{\mathbf{n}} = \mathbf{r}/r$. The entire orbital plane then precesses around the total momentum in the direction $\hat{\Psi}$ given by

$$\hat{\Psi} = \hat{\mathbf{J}} \times \frac{(\hat{\mathbf{J}} \times \hat{\mathbf{L}})}{|\hat{\mathbf{J}} \times \hat{\mathbf{L}}|} \quad . \quad (2)$$

In the set of coordinates (r, Φ, Ψ) and their conjugate momenta (P_r, P_Φ, P_Ψ) , the angular conjugate momenta are simply $P_\Phi = L$ and $P_\Psi = L_z = \mathbf{L} \cdot \hat{\mathbf{J}}$. The magnitude of the orbital angular momentum L is conserved and so, therefore, is P_Φ .

In the restricted case of one effective spin – again, defined by one black hole spinning or two equal mass black holes with arbitrary spins – the component of the orbital angular momentum along $\hat{\mathbf{J}}$, and therefore P_Ψ , is also conserved. The Hamiltonian equations of motion then have a remarkably simple form:

$$\begin{aligned} \dot{r} &= \frac{\partial H}{\partial P_r}, \quad \dot{P}_r = -\frac{\partial H}{\partial r} \\ \dot{\Phi} &= \frac{\partial H}{\partial P_\Phi}, \quad \dot{P}_\Phi = 0 \\ \dot{\Psi} &= \frac{\partial H}{\partial P_\Psi}, \quad \dot{P}_\Psi = 0 \end{aligned} \quad (3)$$

The natural frequencies given by radial oscillations, $f_r = 1/T_r$ where T_r is the radial period, periastron precession, $f_\Phi = \dot{\Phi}/2\pi$, and orbital plane precession $f_\Psi = \dot{\Psi}/2\pi$, are functions of r only.

The more general equations, when both black holes spin and have unequal masses, and dissipation is included, are collected in the Appendices. In the coordinate system introduced above, adding a second spin (for unequal mass) renders $P_\Psi = L_z$ no longer conserved, although $P_\Phi = L$ continues to be conserved. Consequently, the precessional frequencies will not depend solely on r , but will be modulated by angular position. Adding dissipation drains both P_Φ and P_Ψ , although (r, Φ, Ψ) remains the natural coordinate system for disentangling the two kinds of precession.

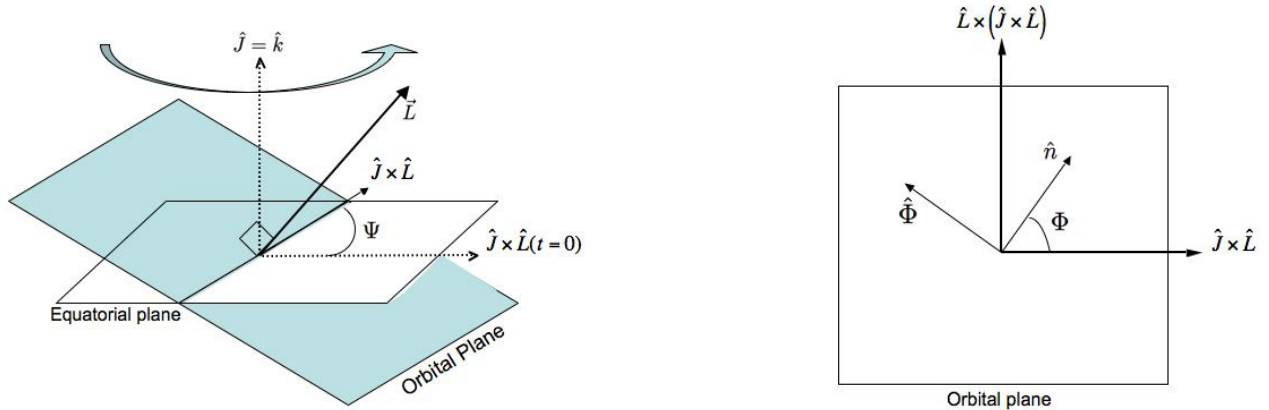


FIG. 2: The orbital plane coordinates as defined in Ref. [19] Fig. 1. Left: The orbital plane spanned by $\mathbf{r} \times \mathbf{p}$ precesses around the total angular momentum with frequency $\dot{\Psi}$. Right: The coordinates as defined within the orbital plane.

We then convert the radiation-reaction terms derived in the Lagrangian formulation (§A) into Hamiltonian variables (§B). We are motivated to show our results in the following section in Hamiltonian variables by the simplicity of Eqs. (3) and the simplicity of the analytic expressions for the frequencies, as we discuss in the following section (see Eqs. (7)). Of course, practitioners are free to choose either the Lagrangian or the Hamiltonian formulation, since both admit equivalent descriptions, so that an orbital-plane decomposition can be found with corresponding frequencies. The Hamiltonian formulation offers a cleaner framework in which to examine the explicit equations, so we favor it slightly for the purposes of the paper.¹

III. GALLERY OF INSPIRALS

Using the equations of motion of §B, we can investigate a completely generic orbit. The most general scenario allows for both black holes to spin and for those spins to be misaligned. These three-dimensional orbits should have three natural frequencies. As described in §II, the natural frequencies are the radial oscillations of an eccentric orbit

$$f_r = \frac{1}{T_r} \quad , \quad (4)$$

¹ For example, the simplicity of $\vec{L} = \vec{r} \times \vec{p}$ in the Hamiltonian formulation renders our geometric interpretation more transparent than the lengthy 3PN corrected definition of \vec{L} in the Lagrangian variables.

where T_r is the time between successive periastra, the frequency of periastron precession in the orbital plane,

$$f_\Phi = \frac{\dot{\Phi}}{2\pi} \quad , \quad (5)$$

and the frequency of plane precession,

$$f_\Psi = \frac{\dot{\Psi}}{2\pi} \quad . \quad (6)$$

In the conservative Hamiltonian system, it was found that if spin-spin contributions were omitted, then [19]

$$\begin{aligned} 2\pi f_\Phi &= \dot{\Phi} = A \frac{L}{r^2} + \frac{\mathbf{S}_{\text{eff}} \cdot \hat{\mathbf{L}}}{r^3} - \dot{\Psi}(\hat{\mathbf{J}} \cdot \hat{\mathbf{L}}) \\ 2\pi f_\Psi &= \dot{\Psi} = \left(\frac{\hat{\mathbf{J}} \times (\mathbf{S}_{\text{eff}} \times \hat{\mathbf{L}})}{|\hat{\mathbf{J}} \times \hat{\mathbf{L}}| r^3} \right) \cdot \hat{\Psi} \end{aligned} \quad (7)$$

where $A = 2 \partial H / \partial \mathbf{p}^2$ (Eq. (B17)), and \mathbf{S}_{eff} is defined in Eq. (B6). Although we add spin-spin coupling, we continue to use Eqs. (7) as adiabatic estimates for the frequencies.

The full waveform will be composed of the frequencies (4)-(6). The waveform is computed to leading quadrupole order, although the orbital variables that go into this expression are computed in the full 3.5PN system,

$$h_{ij} = \frac{2\mu}{D} 2 \left(v_i v_j - \frac{1}{r} \hat{r}_i \hat{r}_j \right) \quad , \quad (8)$$

with D the distance to the sources. This is referred to as the restricted PN waveform approximation. For simplicity, we place the Earth along $\hat{z} = \hat{J}$. For greater precision, higher-order corrections to the amplitude (including spins) have been computed [21, 22], but for our purposes, the leading-order amplitude is sufficient.

A. Quasi-spherical

We now consider quasi-spherical, low eccentricity orbits (see also [23]). Low eccentricity orbits look quasi-circular in the orbital plane. As the orbital plane precesses, these orbits lie on the surface of a sphere whose radius decreases monotonically as gravitational radiation is emitted. We work in the Hamiltonian formulation, since the Hamiltonian better lends itself to finding constant radius orbits and facilitates the geometric breakdown in terms of the orbital plane. Of course, this procedure can readily be repeated in the Lagrangian

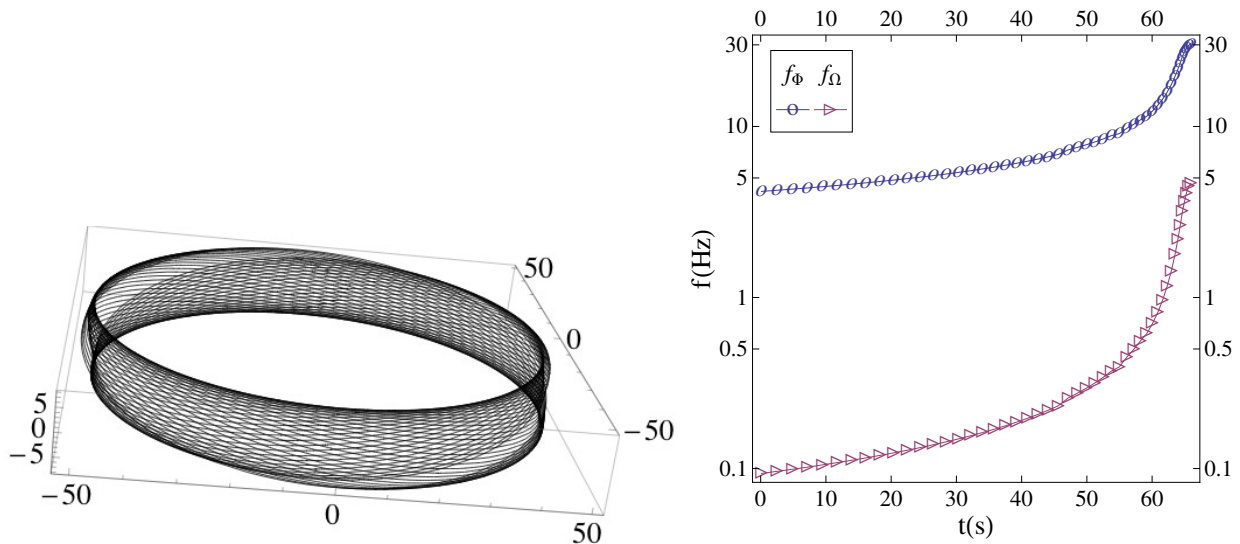


FIG. 3: The initial conditions are set to those of the constant radius orbit at $r_i = 50$ in the absence of spin-spin coupling for an equal mass binary with maximal spins, and spin angles $\theta_1 = \theta_2 = 45^\circ$. Left: The first 10 sec of the orbit is shown (length measured in units of $GM/c^2 \simeq 26.5(M/20M_\odot)\text{km}$). Right: The frequency in the orbital plane as defined in Eq. (7) marked with open circles, and the frequency of plane precession, as defined in Eq. (7), marked with crosses. Both are shown versus time over the entire inspiral. We plot frequencies in units of $(20M_\odot/M)\text{Hz}$ and time in units of $(M/20M_\odot)\text{sec}$.

formulation. We find the constant radius orbit according to the prescription in [19] (see also [23]). We sketch the argument here. The Hamiltonian of Eqs. (B3) and (B4) does not admit a simple effective potential formulation since it is a complicated function of \mathbf{p}^2 . Nonetheless, we can still use the Hamiltonian as an effective potential *at the turning points* if we exclude spin-spin coupling:

$$V_{\text{eff}} = H(P_r = 0) \quad , \quad (9)$$

With this condition, we can find the L of an orbit at a given constant radius. Fixing the initial conditions this way and including spin-spin couplings, we can estimate the deviation away from quasi-sphericity. We find that the oscillations in the radius due to spin-spin coupling are negligible (less than a few percent) and that the radius quickly begins a monotonic decrease as gravitational waves are radiated. Therefore, the spin-spin effect seems to be too small to induce measurable eccentricity during the inspiral if no eccentricity is present initially.

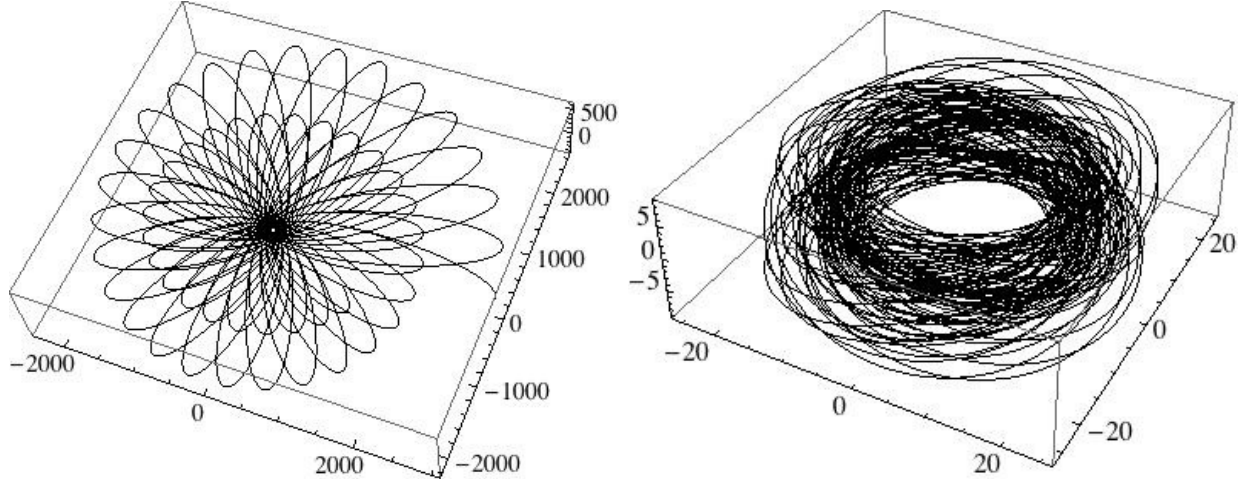


FIG. 4: The pair has $m_2/m_1 = 1/4$, maximal spins, $a_1 = a_2 = 1$, and initial spin angles $\theta_1 = 45^\circ, \theta_2 = 45^\circ$ and initial values $r_i = 3000$ and $L_i = 0.003r_i$. Left: The first 1150s of the inspiral. Right: The final 5s before cutoff.

As an example, consider an equal mass pair with maximal spins $a_1 = a_2 = 1$, and spin angles initially misaligned so that $\theta_1 \equiv \arccos(\hat{\mathbf{L}} \cdot \hat{\mathbf{S}}_1) = 45^\circ$ and $\theta_2 \equiv \arccos(\hat{\mathbf{L}} \cdot \hat{\mathbf{S}}_2) = 45^\circ$. This is shown in Fig. 3, where the first ten seconds of the total orbit is shown. The full orbit takes ~ 60 seconds to merge for $M = 20M_\odot$. We take the initial condition to be $r_i = 50$ and set L initially at the quasi-spherical value determined by Eq. (9). The natural frequencies f_Φ and f_Ψ are shown in the right panel. Since the orbit is quasi-spherical, the frequency of radial oscillations f_r is not informative. Periastron precession dominates over plane precession, $f_\Phi > f_\Psi$, which is expected since plane precession is a higher-order effect.

Using physical units, with the initial separation of $r_i \sim 50$, the gravitational radiation has an initial frequency

$$2 \times f_\Phi \sim 9.5\text{Hz} \left(\frac{20M_\odot}{M} \right) \quad (10)$$

which is already nearing the Advanced LIGO/VIRGO band for two $10M_\odot$ black holes, and is sweeping through the bandwidth as the orbital separation decreases. The much slower frequency of precession, f_Ψ , does not have a significant effect on the waveform for the quasi-spherical case.

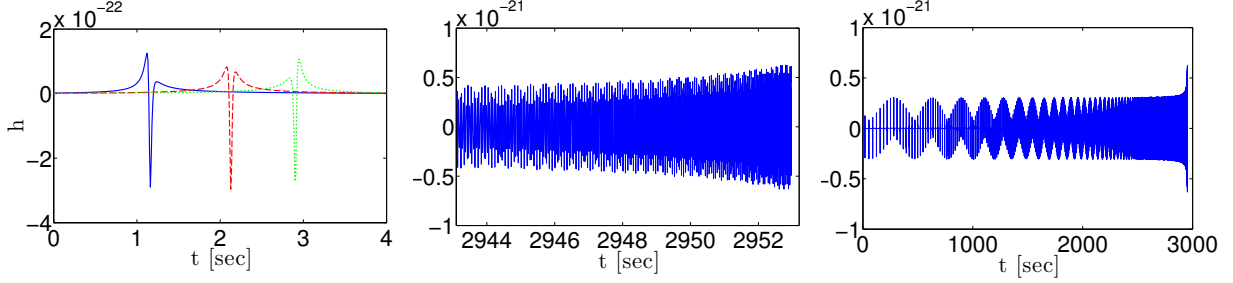


FIG. 5: Strain for an optimally-oriented binary with $M = 20M_{\odot}$ at $D = 100$ Mpc. From left to right, we show three periastron passes occurring ~ 3000 sec prior to waveform truncation (shifted in time by ~ 34 sec each to increase their overlap), the final 10 seconds, and the final ~ 3000 seconds of the waveform.

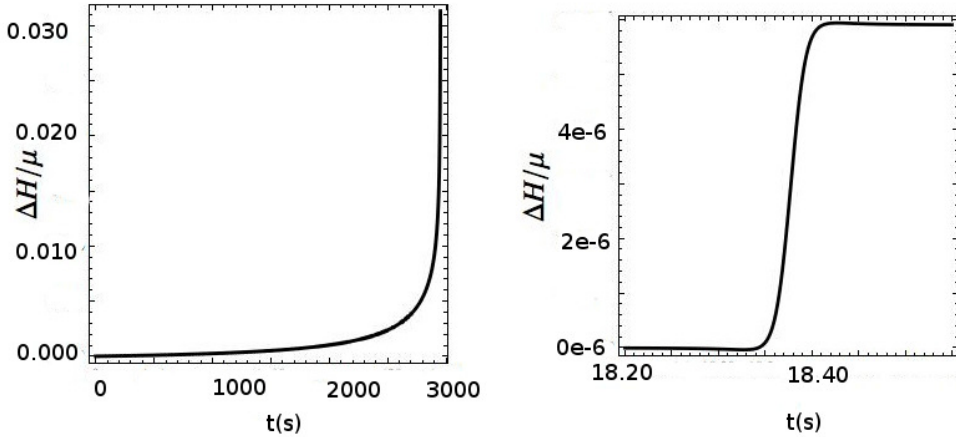


FIG. 6: ΔH is the absolute value of the difference between the energy as a function of time and the initial energy. Left: The burst of energy emitted during one periastron passage ($r_p \sim 38$). As the pair separate to apastron $r_a \sim 3000$, negligible energy is lost as confirmed by the flatness of ΔH . Each burst is small although a few percent of the total energy in μ is lost cumulatively prior to cutoff as shown on the right.

B. Eccentric, unequal masses

We next consider an eccentric pair with mass ratio $m_1/m_2 = 1/4$. Each black hole is spinning maximally. Both spins are misaligned with the orbital plane with $\theta_1 \equiv \arccos(\hat{\mathbf{L}} \cdot \hat{\mathbf{S}}_1) = 45^\circ$ and $\theta_2 \equiv \arccos(\hat{\mathbf{L}} \cdot \hat{\mathbf{S}}_2) = 45^\circ$. The pair begins at large separation, $r_i = 3000$, and with angular momentum $L = 0.003r_i$. The first periastron passage is $r_p \sim 38$, so the

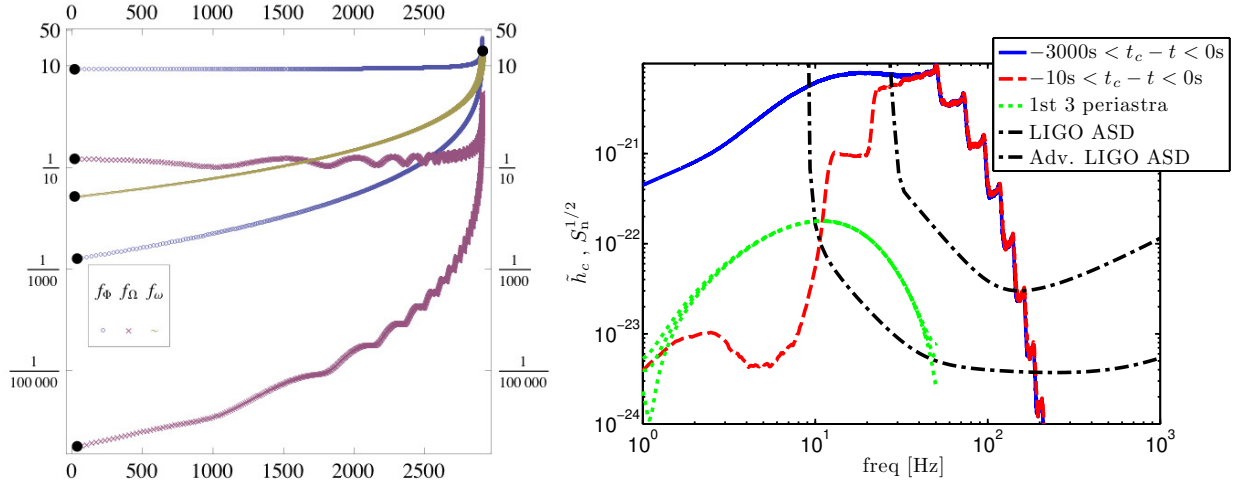


FIG. 7: Left: The three natural frequencies versus time for the eccentric configuration. There are two lines for f_Φ , one marking the value at periastron (top line) and the other marking the value at apastron (bottom line). Same for f_Ψ . All frequencies are plotted in units of $(20M_\odot/M)\text{Hz}$ and all times in units of $(M/20M_\odot)\text{sec}$. Right: The characteristic strain, h_c , of an optimally-oriented realization of the eccentric configuration, at a distance of 100 Mpc, again scaled for $M = 20M_\odot$. We show h_c for each of the first three periastron passages, the final 100 sec, and the entire 3000 sec intervals shown in Fig. 5. We show the LIGO and Advanced LIGO sensitivity curves [24] for comparison.

pair is set on a highly eccentric orbit. The eccentricity can be defined loosely as

$$e = \frac{r_a - r_p}{r_a + r_p} \quad (11)$$

where r_a is the apastron and r_p is the periastron. The eccentricity begins large, $e = 0.97$, and drifts down to $e = 0.17$ by the time the simulation is ended. Cutoff is set when the 3.5PN terms become larger than the 2.5PN terms, or, equivalently, when $\dot{E} > 0$, as we discuss in the next section. At cutoff, the periastron is $r_p \sim 12$ and the apastron is $r_a \sim 17$. Our choice of the initial pericenter distance and eccentricity is consistent with the capture formation scenario of stellar mass black hole binaries in globular clusters [14]. Therefore, an initially highly eccentric orbit could retain significant eccentricity by the time it evolves into the bandwidth of a terrestrial network of gravitational-wave interferometers.

The pair experiences both periastron precession and orbital-plane precession during a total of 1384 orbits, some of which are shown in Fig. 4. On the left of Fig. 4 the first 1150s of the orbit are shown and on the right the final 5s of the orbit is shown before the

simulation is cutoff. Both the precession of the periastron and the precession of the orbital plane are apparent in Fig. 4. The precession of the orbital plane is more prominent the more disparate the masses of the black holes. While spin precession remains substantial to the end, periastron precession becomes less significant as eccentricity is shed.

Since the orbit is highly eccentric, a burst of gravitational radiation is emitted near periastron passage as shown in Fig. 5. During the most eccentric cycles, the bursts are what one might expect from a parabolic encounter, with energy and angular momentum losses occurring primarily near periastron. A tiny amount of energy is emitted per periastron passage for the $M = 20M_\odot$ pair shown in Fig. 6, although a few percent of the total μ is shed prior to plunge. The bursty waveform is highly distinct from the extremely regular quasi-circular waveforms, clearly showing effects of the precession.

The natural frequencies $f_\Phi > f_r > f_\Psi$ are shown on the left of Fig. 7. Both f_Φ and f_Ψ are shown only at periastron (top line) and apastron (bottom). Therefore, there are two lines each for f_Φ and f_Ψ . The value of the frequencies at apastron is much smaller than at periastron if the eccentricity is large. These discrete values approach each other as the eccentricity decreases. Since T_r is defined as the time between successive perihelia, there is only one line for $f_r = 1/T_r$. The wobbling in f_Ψ is a result of spin-spin coupling. The time between bursts is given by the radial period, $T_r = 1/f_r$, and the frequency of the burst is given by f_Φ at periastron passage during the highly-eccentric, nearly parabolic encounter, and by $2 \times f_\Phi$ when the orbit is less eccentric.

The right panel of Fig. 7 shows the characteristic strain,

$$h_c \equiv 2f \sqrt{|\tilde{h}_+|^2 + |\tilde{h}_x|^2}, \quad (12)$$

for the three time intervals shown in Fig. 5, as well as the noise amplitude spectral densities for the initial and Advanced LIGO detectors. The self-similarity of the periastron passages is evident in Fig. 7. We suggest the possibility that this self-similarity could be employed to coherently combine the signals from all the periastron passages of a highly eccentric system, while ignoring the data in between where the signal power is negligible.

The characteristic strain of the full signal has a flat plateau that spans the frequency range between the spin precession frequency and twice the orbital frequency, both evaluated at periastron, because the power emitted during each orbit is dominated by the emission at periastron. The characteristic strain of the final 10 sec shows a very clear step structure

due to the large set of harmonics excited by the eccentric motion. We emphasize that these harmonics are not the instantaneous harmonics from PN corrections, as we have not included higher-harmonic PN corrections. Rather, the harmonics apparent in Fig. 7 are the result of the large change in instantaneous frequency over the course of each orbit, which is represented in Fourier space as higher (and lower) harmonics of twice the mean orbital frequency. Again, the highest plateau spans between the spin precession frequency and twice the orbital frequency, with the step at lower frequency occurring at the orbital frequency, and the many steps at higher frequencies occurring at larger integer multiples of the orbital frequency.

IV. DOMAIN OF VALIDITY FOR THE PN APPROXIMATION

The PN equations of motion are a series expansion of corrections to the acceleration of the binary components, with whole order terms representing conservative, relativistic corrections, and half order terms representing dissipative corrections. As such, the expansion should not be trusted when higher-order terms become comparable in magnitude to lower-order terms. In this regard, it is noteworthy that the sign of the acceleration term along the radial direction is negative at 2.5PN order, as expected, and the black holes are drawn together. However, the sign of the acceleration term along the radial direction is positive at 3.5PN order. In other words, the 2.5PN terms over estimate the effects of dissipation, and the 3.5PN terms temper this over estimate. A consequence of the breakdown of the PN expansion in the strong-field regime is that the 3.5PN term comes to dominate, and spuriously drives the system to a larger separation, with the 3.5PN term acting as a source, rather than a sink, of energy and angular momentum. Implementation of the equations of motion must be cut off before this happens, as the PN approximation has already broken down at this point. We find that the break down tends to happen at radial separations $r \sim 10$ in units of the total mass, which is well outside the Schwarzschild ISCO at $6M$ that is frequently used to represent the boundary for a valid application of the PN expansion.

All of the simulations in the preceding section are therefore cut off when the PN approximation begins to break down. Specifically, we use the criterion that the simulation ends when the rate of energy loss drops below some threshold, indicating that the 3.5PN correction is approaching the same magnitude as the 2.5PN term. In Fig. 8, we show the relative

magnitude of different PN-order contributions to the (Lagrangian) equations of motion. We focus on two cases: an equal mass, nonspinning binary undergoing quasi-circular inspiral, and our eccentric configuration from the previous section. The first case is likely to be a best-case scenario for the convergence of the PN expansion, while the latter is likely to over extend the PN expansion at larger orbital separations. We find that, for the conservative terms, the ratio of adjacent whole-order terms in the PN sequence remains less than unity over the full domain, and indeed would remain so down to the aforementioned ISCO radius. However, the ratio of the two half order, dissipative terms exceeds unity at $r = 9.125M$ in the circular case, and at $r = 10M$ in the eccentric spinning case. Since the approximation is certainly unreliable prior to the point where this ratio equals unity, we suggest that generally the PN expansion cannot be reliably applied for separations $r \lesssim 10M$ for any configuration when dissipation is included.

Another possibility is that the optimal asymptotic expansion for the PN sequence should be truncated at 3 PN order. This is an interesting possibility, and would in fact be consistent with findings in the Schwarzschild test-mass limit, where much higher PN terms are available to demonstrate this behavior [25]. Since for comparable masses we lack higher PN-order terms, it is not yet possible to distinguish between these two possibilities.

V. SUMMARY

We have compiled the equations of motion of Refs. [8–11], and have transformed them into Hamiltonian coordinates for ready-to-use equations governing general black hole binaries. With these in hand, we can study any black hole pair, including the effects of spin, eccentricity, and their accompanying precessions. Given this flexible system, we have answered four basic questions:

- ‘Do spinning pairs tend to quasi-spherical orbits?’

We find that the deviation for a constant radius orbit due to spin-spin coupling is insignificantly small, so quasi-spherical orbits are accessible. Consequently spinning pairs do tend to quasi-spherical orbits.

- ‘What features are generically introduced into waveforms through periastron and spin precession?’

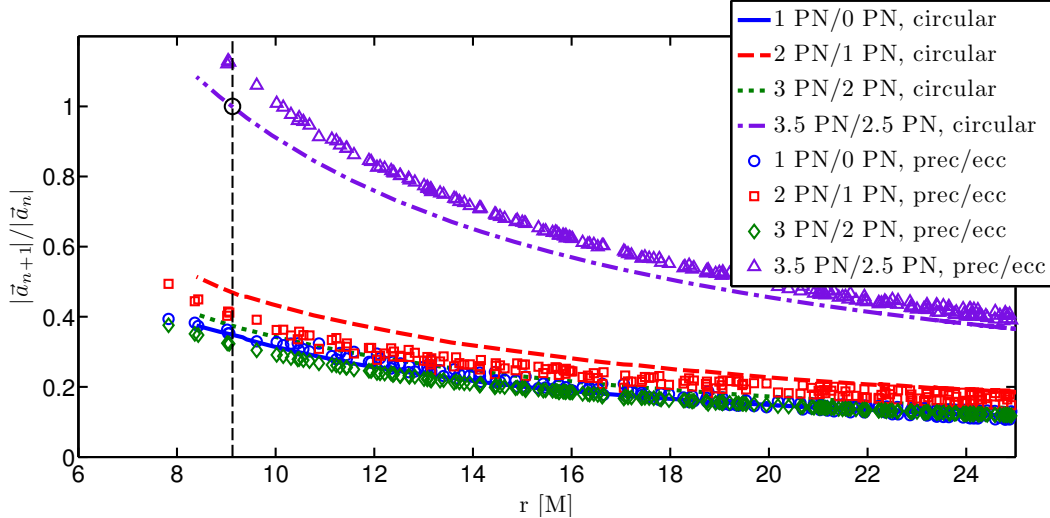


FIG. 8: The ratio of different PN-order contributions to the Lagrangian equations of motion for a circular, equal mass, nonspinning inspiral, and separately for our eccentric configuration. Even for the circular case, the 3.5 PN dissipation term grows larger than the 2.5 PN dissipation term for radial separations less than $\sim 9M$. Less ideal cases, not surprisingly, appear to make the PN sequence diverge at larger radii.

As was shown in [19], an orbit can be projected onto an orbital plane. The characteristic frequency within the plane supplants the usual coordinate frequency. The frequency of plane precession and the frequency of radial oscillations provide the other crucial frequencies for analysis. We have shown that these three frequencies leave a characteristic imprint on the waveforms in Fourier space. Furthermore, the frequency of bursts for highly eccentric orbits and the quiescent time between bursts directly reflect these natural harmonics and could encourage novel data analysis techniques.

- ‘How much energy is lost during each burst near periastron passage?’

Given the caveat that most of the energy will be lost during the merger, which is beyond the reach of the PN approximation, for highly eccentric binaries we show that less than 10^{-3} of a percent of the reduced mass μ is lost to gravitational radiation per periastron passage. Some pairs may execute thousands of orbits before plunge so that a few percent of μ is lost during inspiral up to $r \sim 10M$.

- ‘How much of the orbit and waveform for eccentric, precessing orbits is well described by the PN expansion?’

The PN expansion has broken down whenever higher-order corrections become larger than lower-order corrections. We find this tends to happen at $r \sim 10M$, which is well outside of the Schwarzschild ISCO that is often used to demarcate the breaking point of the PN approximation. Possibly the PN sequence diverges inside $\sim 10M$, or it may be that the optimal PN expansion inside this radius should be truncated at no higher than 3 PN order.

The orbits shown give a sample of the complete range that can be probed in detail for generic, spinning, precessing, eccentric black hole pairs. We intend to build a data set of black hole pairs to be made available as a testing ground for developing data analysis techniques.

Acknowledgements

We are grateful to Clifford Will for his invaluable insights and to Jameson Rollins for important conversations. This work was supported by an NSF grant AST-0908365. JL gratefully acknowledges support of a KITP Scholarship, under Grant no. NSF PHY05-51164.

Appendix A: Lagrangian Equations of Motion

In this section we compile the equations of motion including spin couplings and dissipation as computed by Will and collaborators over the series of papers [8–11]. We measure length in units of total mass $M = m_1 + m_2$ and write the equations in terms of the dimensionless center-of-mass coordinate \mathbf{x} and center-of-mass velocity \mathbf{v} . The reduced mass is defined as $\eta = \mu/M = m_1 m_2 / M^2$. The Lagrangian equations of motion in \mathbf{x}, \mathbf{v} with spins added are (with $x = \sqrt{\mathbf{x} \cdot \mathbf{x}}$ the harmonic radial coordinate and $\dot{x} = \hat{\mathbf{n}} \cdot \mathbf{v}$) as compiled from Refs. [8, 9, 21, 22]

$$\dot{\mathbf{x}} = \mathbf{v} \tag{A1}$$

$$\ddot{\mathbf{x}} = \mathbf{a}_N + \mathbf{a}_{1PN} + \mathbf{a}_{2PN} + \mathbf{a}_{2.5PN} + \mathbf{a}_{3PN} + \mathbf{a}_{3.5PN} + \mathbf{a}_{PN-SO} + \mathbf{a}_{3.5PN-SO} + \mathbf{a}_{PN-SS} + \mathbf{a}_{3.5PN-SS}$$

and

$$\begin{aligned}
\mathbf{a}_N &= -\frac{\hat{\mathbf{n}}}{x^2} \\
\mathbf{a}_{1PN} &= -\frac{\hat{\mathbf{n}}}{x^2} \left\{ (1 + 3\eta)\mathbf{v}^2 - 2(2 + \eta)\frac{1}{x} - \frac{3}{2}\eta\dot{x}^2 \right\} + \frac{\mathbf{v}}{x^2} 2(2 - \eta)\dot{x} \\
\mathbf{a}_{2PN} &= -\frac{\hat{\mathbf{n}}}{x^2} \left\{ \frac{3}{4}(12 + 29\eta)\frac{1}{x^2} + \eta(3 - 4\eta)(\mathbf{v}^2)^2 + \frac{15}{8}\eta(1 - 3\eta)\dot{x}^4 \right. \\
&\quad \left. - \frac{3}{2}\eta(3 - 4\eta)\mathbf{v}^2\dot{x}^2 - \frac{1}{2}\eta(13 - 4\eta)\frac{\mathbf{v}^2}{x} - (2 + 25\eta + 2\eta^2)\frac{\dot{x}^2}{x} \right\} \\
&\quad + \frac{\mathbf{v}}{x^2} \left\{ \frac{\dot{x}}{2} \left[\eta(15 + 4\eta)\mathbf{v}^2 - (4 + 41\eta + 8\eta^2)\frac{1}{x} - 3\eta(3 + 2\eta)\dot{x}^2 \right] \right\} . \\
\mathbf{a}_{2.5PN} &= \frac{\hat{\mathbf{n}}}{x^2} \left\{ \frac{8}{5}\eta \left(\frac{1}{x} \right) \dot{x} \left(\frac{17}{3} \frac{1}{x} + 3v^2 \right) \right\} \\
&\quad - \frac{\mathbf{v}}{x^2} \left\{ \frac{8}{5}\eta \left(\frac{1}{x} \right) \left(3\frac{1}{x} + v^2 \right) \right\} . \\
\mathbf{a}_{3PN} &= -\frac{\hat{\mathbf{n}}}{x^2} \left\{ - \left[16 + \left(\frac{1399}{12} - \frac{41}{16}\pi^2 \right) \eta + \frac{71}{2}\eta^2 \right] \left(\frac{1}{x} \right)^3 - \eta \left[\frac{20827}{840} + \frac{123}{64}\pi^2 - \eta^2 \right] \left(\frac{1}{x} \right)^2 v^2 \right. \\
&\quad + \left[1 + \left(\frac{22717}{168} + \frac{615}{64}\pi^2 \right) \eta + \frac{11}{8}\eta^2 - 7\eta^3 \right] \left(\frac{1}{x} \right)^2 \dot{x}^2 \\
&\quad + \frac{\eta}{4} (11 - 49\eta + 52\eta^2) v^6 - \frac{35}{16}\eta(1 - 5\eta + 5\eta^2)\dot{x}^6 + \frac{\eta}{4} (75 + 32\eta - 40\eta^2) \left(\frac{1}{x} \right) v^4 \\
&\quad + \frac{\eta}{2} (158 - 69\eta - 60\eta^2) \left(\frac{1}{x} \right) \dot{x}^4 - \eta (121 - 16\eta - 20\eta^2) \left(\frac{1}{x} \right) v^2 \dot{x}^2 \\
&\quad \left. - \frac{3}{8}\eta (20 - 79\eta + 60\eta^2) v^4 \dot{x}^2 + \frac{15}{8}\eta (4 - 18\eta + 17\eta^2) v^2 \dot{x}^4 \right\} \\
&\quad + \frac{\mathbf{v}}{x^2} \dot{x} \left\{ \left[4 + \left(\frac{5849}{840} + \frac{123}{32}\pi^2 \right) \eta - 25\eta^2 - 8\eta^3 \right] \left(\frac{1}{x} \right)^2 + \frac{\eta}{8} (65 - 152\eta - 48\eta^2) v^4 \right. \\
&\quad + \frac{15}{8}\eta (3 - 8\eta - 2\eta^2) \dot{x}^4 + \eta (15 + 27\eta + 10\eta^2) \left(\frac{1}{x} \right) v^2 \\
&\quad \left. - \frac{\eta}{6} (329 + 177\eta + 108\eta^2) \left(\frac{1}{x} \right) \dot{x}^2 - \frac{3}{4}\eta (16 - 37\eta - 16\eta^2) v^2 \dot{x}^2 \right\}
\end{aligned}$$

$$\begin{aligned}
\mathbf{a}_{3.5PN} = & -\frac{\hat{\mathbf{n}}}{x^2} \left\{ \frac{8}{5}\eta \left(\frac{1}{x}\right) \dot{x} \left[\frac{23}{14}(43 + 14\eta) \left(\frac{1}{x}\right)^2 + \frac{3}{28}(61 + 70\eta)v^4 + 70\dot{x}^4 \right. \right. \\
& \left. \left. + \frac{1}{42}(519 - 1267\eta) \left(\frac{1}{x}\right) v^2 + \frac{1}{4}(147 + 188\eta) \left(\frac{1}{x}\right) \dot{x}^2 - \frac{15}{4}(19 + 2\eta) v^2 \dot{x}^2 \right] \right\} \\
& + \frac{\mathbf{v}}{x^2} \left\{ \frac{8}{5}\eta \left(\frac{1}{x}\right) \left[\frac{1}{42}(1325 + 546\eta) \left(\frac{1}{x}\right)^2 + \frac{1}{28}(313 + 42\eta) v^4 + 75\dot{x}^4 \right. \right. \\
& \left. \left. - \frac{1}{42}(205 + 777\eta) \left(\frac{1}{x}\right) v^2 + \frac{1}{12}(205 + 424\eta) \left(\frac{1}{x}\right) \dot{x}^2 - \frac{3}{4}(113 + 2\eta) v^2 \dot{x}^2 \right] \right\} .
\end{aligned} \tag{A2}$$

using the 3PN and half-order terms from Ref. [9].

We also absorb an M^2 into the spins so the physical spin in the Lagrangian system is denoted $\mathcal{S}_i = a_i(m_i^2/M^2)$ where a_i is the dimensionless amplitude $0 \leq |a_i| \leq 1$. As we will see in §B, this is a different normalization from that for spins in the Hamiltonian case, where spins are expressed as $\mathbf{S}_i = a_i(m_i^2/\mu M)$. The spin-orbit contribution to the acceleration is

$$\mathbf{a}_{PN-SO} = \frac{1}{x^3} \left\{ 6\frac{\hat{\mathbf{n}}}{x} \tilde{\mathbf{L}}_N \cdot (\mathcal{S} + \xi) - \mathbf{v} \times (4\mathcal{S} + 3\xi) + 3\dot{x}\hat{\mathbf{n}} \times (2\mathcal{S} + \xi) \right\}$$

with $\xi \equiv (m_2/m_1)\mathcal{S}_1 + (m_1/m_2)\mathcal{S}_2$ [10]. It is customary to define a *reduced* Newtonian orbital angular momentum,

$$\tilde{\mathbf{L}}_N = \mathbf{x} \times \mathbf{v} . \tag{A3}$$

The spin-orbit dissipation term with the covariant spin supplementary condition is (see the appendix of Ref. [10]),

$$\begin{aligned}
\mathbf{a}_{3.5PN-SO} = & -\frac{\eta}{5x^4} \left\{ \frac{\dot{x}\hat{\mathbf{n}}}{x} \left[\left(120v^2 + 280\dot{x}^2 + 453\frac{1}{x} \right) \tilde{\mathbf{L}}_N \cdot \mathcal{S} \right. \right. \\
& \left. \left. + \left(120v^2 + 280\dot{x}^2 + 458\frac{1}{x} \right) \tilde{\mathbf{L}}_N \cdot \xi \right] \right. \\
& \left. + \frac{\mathbf{v}}{x} \left[\left(87v^2 - 675\dot{x}^2 - \frac{901}{3}\frac{1}{x} \right) \tilde{\mathbf{L}}_N \cdot \mathcal{S} + 4 \left(18v^2 - 150\dot{x}^2 - 66\frac{1}{x} \right) \tilde{\mathbf{L}}_N \cdot \xi \right] \right. \\
& \left. - \frac{2}{3}\dot{x}\mathbf{v} \times \mathcal{S} \left(48v^2 + 15\dot{x}^2 + 364\frac{1}{x} \right) + \frac{1}{3}\dot{x}\mathbf{v} \times \xi \left(291v^2 - 705\dot{x}^2 - 772\frac{1}{x} \right) \right. \\
& \left. + \frac{1}{2}\hat{\mathbf{n}} \times \mathcal{S} \left(31v^4 - 260v^2\dot{x}^2 + 245\dot{x}^4 - \frac{689}{3}v^2\frac{1}{x} + 537\dot{x}^2\frac{1}{x} + \frac{4}{3}\frac{1}{x^2} \right) \right. \\
& \left. + \frac{1}{2}\hat{\mathbf{n}} \times \xi \left(115v^4 - 1130v^2\dot{x}^2 + 1295\dot{x}^4 - \frac{869}{3}v^2\frac{1}{x} + 849\dot{x}^2\frac{1}{x} + \frac{44}{3}\frac{1}{x^2} \right) \right\} .
\end{aligned} \tag{A4}$$

And the spin-spin contribution is

$$\mathbf{a}_{PN-SS} = -\frac{3}{\mu x^4} [\hat{\mathbf{n}}(\mathcal{S}_1 \cdot \mathcal{S}_2) + \mathcal{S}_1(\hat{\mathbf{n}} \cdot \mathcal{S}_2) + \mathcal{S}_2(\hat{\mathbf{n}} \cdot \mathcal{S}_1) - 5\hat{\mathbf{n}}(\hat{\mathbf{n}} \cdot \mathcal{S}_1)(\hat{\mathbf{n}} \cdot \mathcal{S}_2)] \quad (\text{A5})$$

See also [22]. The 3.5PN order effects of Spin-Spin coupling from Ref. [11] are

$$\begin{aligned} \mathbf{a}_{3.5PN-SS} = & \frac{1}{x^5} \left\{ \hat{\mathbf{n}} \left[\left(287\dot{x}^2 - 99v^2 + \frac{541}{5} \frac{1}{x} \right) \dot{x}(\mathcal{S}_1 \cdot \mathcal{S}_2) - \left(2646\dot{x}^2 - 714v^2 + \frac{1961}{5} \frac{1}{x} \right) \dot{x}(\hat{\mathbf{n}} \cdot \mathcal{S}_1)(\hat{\mathbf{n}} \cdot \mathcal{S}_2) \right. \right. \\ & \left. \left. + \left(1029\dot{x}^2 - 123v^2 + \frac{629}{10} \frac{1}{x} \right) ((\hat{\mathbf{n}} \cdot \mathcal{S}_1)(\mathbf{v} \cdot \mathcal{S}_2) + (\hat{\mathbf{n}} \cdot \mathcal{S}_2)(\mathbf{v} \cdot \mathcal{S}_1)) - 336\dot{x}(\mathbf{v} \cdot \mathcal{S}_1)(\mathbf{v} \cdot \mathcal{S}_2) \right] \right. \\ & \left. + \mathbf{v} \left[\left(\frac{171}{5} v^2 - 195\dot{x}^2 - 67 \frac{1}{x} \right) (\mathcal{S}_1 \cdot \mathcal{S}_2) - \left(174v^2 - 1386\dot{x}^2 - \frac{1038}{5} \frac{1}{x} \right) (\hat{\mathbf{n}} \cdot \mathcal{S}_1)(\hat{\mathbf{n}} \cdot \mathcal{S}_2) \right. \right. \\ & \left. \left. - 438\dot{x}((\hat{\mathbf{n}} \cdot \mathcal{S}_1)(\mathbf{v} \cdot \mathcal{S}_2) + (\hat{\mathbf{n}} \cdot \mathcal{S}_2)(\mathbf{v} \cdot \mathcal{S}_1)) + 96(\mathbf{v} \cdot \mathcal{S}_1)(\mathbf{v} \cdot \mathcal{S}_2) \right] \right. \\ & \left. + \left(\frac{27}{10} v^2 - \frac{75}{2} \dot{x}^2 - \frac{509}{30} \frac{1}{x} \right) ((\mathbf{v} \cdot \mathcal{S}_2)\mathcal{S}_1 + (\mathbf{v} \cdot \mathcal{S}_1)\mathcal{S}_2) \right. \\ & \left. + \left(\frac{15}{2} v^2 + \frac{77}{2} \dot{x}^2 + \frac{199}{10} \frac{1}{x} \right) \dot{x}((\hat{\mathbf{n}} \cdot \mathcal{S}_2)\mathcal{S}_1 + (\hat{\mathbf{n}} \cdot \mathcal{S}_1)\mathcal{S}_2) \right\} . \quad (\text{A6}) \end{aligned}$$

The spin supplementary condition has no effect on spin-spin terms up to this order. We have not yet included the quadrupole-monopole contribution. Finally, the spins precess according to

$$\begin{aligned} \dot{\mathcal{S}}_1 &= \eta \frac{(\mathbf{x} \times \mathbf{v}) \times \mathcal{S}_1}{x^3} \left(2 + \frac{3m_2}{2m_1} \right) \\ \dot{\mathcal{S}}_2 &= \eta \frac{(\mathbf{x} \times \mathbf{v}) \times \mathcal{S}_2}{x^3} \left(2 + \frac{3m_1}{2m_2} \right) . \quad (\text{A7}) \end{aligned}$$

We could also add to the right hand side of (A7) the spin-spin terms:

$$(\dot{\mathcal{S}}_1)_{PN-SS} = -\frac{1}{x^3} (\mathcal{S}_2 - 3(\hat{\mathbf{n}} \cdot \mathcal{S}_2)\hat{\mathbf{n}}) \times \mathcal{S}_1 \quad (\text{A8})$$

[22] and

$$(\dot{\mathcal{S}}_1)_{3.5PN-SS} = \frac{\eta}{x^5} \left(\frac{2}{3}(\mathbf{v} \cdot \mathcal{S}_2) + 30\dot{x}(\hat{\mathbf{n}} \cdot \mathcal{S}_2) \right) (\hat{\mathbf{n}} \times \mathcal{S}_1) \quad (\text{A9})$$

[11]. Equations (A1)-(A9) constitute the Lagrangian dynamical system. These equations are complete through 3.5PN order except for the spin contributions, for which additional terms have been calculated (see for instance Ref. [26, 27]). Since spin effects are already small at the order we include here, we have not pursued inclusion of the higher- order spin terms.

Notice these spins are not reduced by μ and a definition of dimensionful angular momentum will have a μ in it: $\mathbf{J} = \mu \tilde{\mathbf{L}}_N + \dots + \mathcal{S}_1 + \mathcal{S}_2$.

Next we re-express the dissipation terms in the language of the Hamiltonian system.

Appendix B: Hamiltonian Equations of Motion: Including Dissipation

The Hamiltonian PN-formulation is by definition conservative and therefore does not incorporate dissipation [1–6]. We can, however, take the half-order acceleration terms from the Lagrangian coordinates and simply convert them to the coordinates appropriate for the Hamiltonian. We begin by first laying out the whole-order terms in the usual Hamiltonian system [1–6].

In a Hamiltonian formulation, the equations of motion are derived from

$$\dot{\mathbf{r}} = \frac{\partial H}{\partial \mathbf{p}} \quad , \quad \dot{\mathbf{p}} = -\frac{\partial H}{\partial \mathbf{r}} \quad . \quad (\text{B1})$$

As is standard convention, we work in dimensionless coordinates: the dimensionless coordinate vector, \mathbf{r} , is measured in units of total mass, $M = m_1 + m_2$, for a pair with black hole masses m_1 and m_2 . The canonical momentum, \mathbf{p} , is measured in units of the reduced mass, $\mu = m_1 m_2 / M$. The dimensionless combination $\eta = \mu / M$ will again prove useful. We write vector quantities in bold. The coordinate r is to be understood as the magnitude $r = \sqrt{\mathbf{r} \cdot \mathbf{r}}$. Unit vectors such as $\hat{\mathbf{n}} = \mathbf{r} / r$ will additionally carry a hat. Finally, we have used the dimensionless reduced Hamiltonian $H = \mathcal{H} / \mu$ in Eqs. (B1), where \mathcal{H} is the physical Hamiltonian, to 3PN order plus spin-orbit terms [1–6]. H can be expanded as

$$H = H_N + H_{1PN} + H_{2PN} + H_{3PN} + H_{SO} + H_{SS} \quad , \quad (\text{B2})$$

where

$$\begin{aligned}
H_N &= \frac{\mathbf{p}^2}{2} - \frac{1}{r} & (B3) \\
H_{1PN} &= \frac{1}{8} (3\eta - 1) (\mathbf{p}^2)^2 - \frac{1}{2} [(3 + \eta) \mathbf{p}^2 + \eta(\hat{\mathbf{n}} \cdot \mathbf{p})^2] \frac{1}{r} + \frac{1}{2r^2} \\
H_{2PN} &= \frac{1}{16} (1 - 5\eta + 5\eta^2) (\mathbf{p}^2)^3 + \frac{1}{8} [(5 - 20\eta - 3\eta^2) (\mathbf{p}^2)^2 \\
&\quad - 2\eta^2(\hat{\mathbf{n}} \cdot \mathbf{p})^2 \mathbf{p}^2 - 3\eta^2(\hat{\mathbf{n}} \cdot \mathbf{p})^4] \frac{1}{r} \\
&\quad + \frac{1}{2} [(5 + 8\eta) \mathbf{p}^2 + 3\eta(\hat{\mathbf{n}} \cdot \mathbf{p})^2] \frac{1}{r^2} - \frac{1}{4} (1 + 3\eta) \frac{1}{r^3} \\
H_{3PN} &= \frac{1}{128} (-5 + 35\eta - 70\eta^2 + 35\eta^3) (\mathbf{p}^2)^4 + \frac{1}{16} [(-7 + 42\eta - 53\eta^2 - 5\eta^3) (\mathbf{p}^2)^3 \\
&\quad + (2 - 3\eta)\eta^2(\hat{\mathbf{n}} \cdot \mathbf{p})^2(\mathbf{p}^2)^2 + 3(1 - \eta)\eta^2(\hat{\mathbf{n}} \cdot \mathbf{p})^4 \mathbf{p}^2 - 5\eta^3(\hat{\mathbf{n}} \cdot \mathbf{p})^6] \frac{1}{r} \\
&\quad + \left[\frac{1}{16} (-27 + 136\eta + 109\eta^2) (\mathbf{p}^2)^2 + \frac{1}{16} (17 + 30\eta)\eta(\hat{\mathbf{n}} \cdot \mathbf{p})^2 \mathbf{p}^2 + \frac{1}{12} (5 + 43\eta)\eta(\hat{\mathbf{n}} \cdot \mathbf{p})^4 \right] \frac{1}{r^2} \\
&\quad + \left\{ \frac{1}{192} [-600 + (3\pi^2 - 1340)\eta - 552\eta^2] \mathbf{p}^2 - \frac{1}{64} (340 + 3\pi^2 + 112\eta) \eta(\hat{\mathbf{n}} \cdot \mathbf{p})^2 \right\} \frac{1}{r^3} \\
&\quad + \frac{1}{96} [12 + (872 - 63\pi^2)\eta] \frac{1}{r^4} \quad , \\
H_{SO} &= \frac{\mathbf{L} \cdot \mathbf{S}_{\text{eff}}}{r^3} \quad . & (B4)
\end{aligned}$$

and adding spin-spin,

$$\begin{aligned}
H_{SS} &= \frac{\mu}{r^3} [3(\mathbf{S}_1 \cdot \hat{\mathbf{n}})(\mathbf{S}_2 \cdot \hat{\mathbf{n}}) - \mathbf{S}_1 \cdot \mathbf{S}_2 + & (B5) \\
&\quad \frac{m_2}{2m_1} (3(\mathbf{S}_1 \cdot \hat{\mathbf{n}})(\mathbf{S}_1 \cdot \hat{\mathbf{n}}) - \mathbf{S}_1 \cdot \mathbf{S}_1) + \frac{m_1}{2m_2} (3(\mathbf{S}_2 \cdot \hat{\mathbf{n}})(\mathbf{S}_2 \cdot \hat{\mathbf{n}}) - \mathbf{S}_2 \cdot \mathbf{S}_2)] \quad .
\end{aligned}$$

Notice that H_{SS} includes S_1^2 and S_2^2 terms. For two spinning black holes \mathbf{S}_{eff} is²

$$\mathbf{S}_{\text{eff}} = \delta_1 \mathbf{S}_1 + \delta_2 \mathbf{S}_2 \quad (B6)$$

where the dimensionless reduced spins are defined as

$$\mathbf{S}_1 = a_1(m_1^2/\mu M), \quad \mathbf{S}_2 = a_2(m_2^2/\mu M). \quad (B7)$$

and

$$\delta_1 \equiv \left(2 + \frac{3m_2}{2m_1} \right) \eta, \quad \delta_2 \equiv \left(2 + \frac{3m_1}{2m_2} \right) \eta. \quad (B8)$$

² The definitions for \mathbf{S}_{eff} can vary in the literature up to an overall constant although the reduced H_{SO} must be the same for all prescriptions.

The dimensionless spin amplitudes are confined to the range $0 \leq a_{1,2} \leq 1$. The spins precess according to

$$\frac{d\mathbf{S}_1}{dt} = \frac{\partial H}{\partial \mathbf{S}_1} \times \mathbf{S}_1 \quad (\text{B9})$$

or

$$\begin{aligned} \dot{\mathbf{S}}_1 &= \delta_1 \frac{\mathbf{L} \times \mathbf{S}_1}{r^3} + \frac{\mu}{r^3} \left[3\hat{\mathbf{n}} \left(\left(\mathbf{S}_2 + \frac{m_2}{m_1} \mathbf{S}_1 \right) \cdot \hat{\mathbf{n}} \right) - \mathbf{S}_2 \right] \times \mathbf{S}_1 \\ \dot{\mathbf{S}}_2 &= \delta_2 \frac{\mathbf{L} \times \mathbf{S}_2}{r^3} + \frac{\mu}{r^3} \left[3\hat{\mathbf{n}} \left(\left(\mathbf{S}_1 + \frac{m_1}{m_2} \mathbf{S}_2 \right) \cdot \hat{\mathbf{n}} \right) - \mathbf{S}_1 \right] \times \mathbf{S}_2 \quad . \end{aligned} \quad (\text{B10})$$

The orbital angular momentum precesses according to

$$\begin{aligned} \dot{\mathbf{L}} &= \dot{\mathbf{r}} \times \mathbf{p} + \mathbf{r} \times \dot{\mathbf{p}} \quad (\text{B11}) \\ &= -\frac{\mathbf{L} \times \mathbf{S}_{\text{eff}}}{r^3} - \frac{\mu}{r^3} \left[3\hat{\mathbf{n}} \left(\left(\mathbf{S}_2 + \frac{m_2}{m_1} \mathbf{S}_1 \right) \cdot \hat{\mathbf{n}} \right) \right] \times \mathbf{S}_1 - \frac{\mu}{r^3} \left[3\hat{\mathbf{n}} \left(\left(\mathbf{S}_1 + \frac{m_1}{m_2} \mathbf{S}_2 \right) \cdot \hat{\mathbf{n}} \right) \right] \times \mathbf{S}_2 \end{aligned}$$

Adding these together, it follows that the total angular momentum $\mathbf{J} = \mathbf{L} + \mathbf{S}_1 + \mathbf{S}_2$ is conserved in the absence of dissipation so that the orbital angular momentum precesses according to

$$\dot{\mathbf{L}} = -\dot{\mathbf{S}}_1 - \dot{\mathbf{S}}_2 \quad . \quad (\text{B12})$$

Now, we are ready to convert the radiation-reaction terms of appendix A into Hamiltonian variables. To do so, we need to relate the Hamiltonian variables (\mathbf{r}, \mathbf{p}) to the Lagrangian variables (\mathbf{x}, \mathbf{v}) . To convert the 2.5PN radiation-reaction term, we only need the 1PN-order coordinate conversion to catch all corrections up to 3.5PN. To convert the 3.5PN radiation-reaction term, we only need the zeroth-order PN coordinate conversion. It has been shown that to 1PN order [?]]

$$\mathbf{r} = \mathbf{x} \quad , \quad (\text{B13})$$

so that

$$\dot{\mathbf{r}} = \dot{\mathbf{x}} = \mathbf{v} \quad . \quad (\text{B14})$$

What we really want are the harmonic variables of the Lagrangian formulation (\mathbf{x}, \mathbf{v}) in terms of canonical Hamiltonian variables (\mathbf{r}, \mathbf{p}) to 1PN order. We have $\mathbf{x}(\mathbf{r}, \mathbf{p})$ above. To find $\mathbf{v}(\mathbf{r}, \mathbf{p})$, we use Hamilton's equations:

$$\begin{aligned} \dot{\mathbf{r}} &= A\mathbf{p} + B\hat{\mathbf{n}} + \frac{\mathbf{S}_{\text{eff}} \times \mathbf{r}}{r^3} \\ \dot{\mathbf{p}} &= C\mathbf{p} + D\hat{\mathbf{n}} + \frac{\mathbf{S}_{\text{eff}} \times \mathbf{p}}{r^3} + \frac{3\hat{\mathbf{n}}}{r} H_{SO} - \frac{\partial H_{SS}}{\partial \mathbf{r}} \quad , \end{aligned} \quad (\text{B15})$$

where A, B, C, D are

$$A \equiv 2 \left. \frac{\partial H_{PN}}{\partial \mathbf{p}^2} \right|_{r, (\hat{\mathbf{n}} \cdot \mathbf{p})} \quad (\text{B16})$$

$$B \equiv \left. \frac{\partial H_{PN}}{\partial (\hat{\mathbf{n}} \cdot \mathbf{p})} \right|_{r, \mathbf{p}}$$

$$C \equiv -\frac{1}{r} \left. \frac{\partial H_{PN}}{\partial (\hat{\mathbf{n}} \cdot \mathbf{p})} \right|_{r, \mathbf{p}} = -\frac{B}{r}$$

$$\begin{aligned} D &\equiv -\left. \frac{\partial H_{PN}}{\partial r} \right|_{\mathbf{p}, (\hat{\mathbf{n}} \cdot \mathbf{p})} + \left. \frac{\partial H_{PN}}{\partial (\hat{\mathbf{n}} \cdot \mathbf{p})} \right|_{r, \mathbf{p}} \frac{(\hat{\mathbf{n}} \cdot \mathbf{p})}{r} \\ &= -\left. \frac{\partial H_{PN}}{\partial r} \right|_{\mathbf{p}, (\hat{\mathbf{n}} \cdot \mathbf{p})} - (\hat{\mathbf{n}} \cdot \mathbf{p})C \quad . \end{aligned} \quad (\text{B17})$$

and $H_{PN} = H_N + H_{1PN} + H_{2PN} + H_{3PN}$. Explicit expressions can be found in [20], but we will only need A and B here to 1PN order to calculate $\mathbf{v}(\mathbf{r}, \mathbf{p})$ to 1PN order and ultimately find the radiative contributions to the accelerations. Taking the appropriate derivatives of the Hamiltonian to 1PN order, we have

$$\begin{aligned} A_{\leq 1PN} &= 1 + \frac{1}{2} (3\eta - 1) \mathbf{p}^2 - (3 + \eta) \frac{1}{r} \\ B_{\leq 1PN} &= -\eta (\hat{\mathbf{n}} \cdot \mathbf{p}) \frac{1}{r} \quad . \end{aligned} \quad (\text{B18})$$

This gives us \mathbf{v} in terms of (\mathbf{r}, \mathbf{p}) :

$$\mathbf{v} = \left(1 + \frac{1}{2} (3\eta - 1) \mathbf{p}^2 - (3 + \eta) \frac{1}{r} \right) \mathbf{p} - \eta (\hat{\mathbf{n}} \cdot \mathbf{p}) \frac{1}{r} \hat{\mathbf{n}} + \frac{\mathbf{S}_{\text{eff}} \times \mathbf{r}}{r^3} \quad (\text{B19})$$

and

$$\begin{aligned} v^2 &= \left(1 + (3\eta - 1) \mathbf{p}^2 - 2(3 + \eta) \frac{1}{r} \right) \mathbf{p}^2 - 2\eta (\hat{\mathbf{n}} \cdot \mathbf{p})^2 \frac{1}{r} + 2 \frac{\mathbf{p} \cdot (\mathbf{S}_{\text{eff}} \times \mathbf{r})}{r^3} \\ &= \left(1 + (3\eta - 1) \mathbf{p}^2 - 2(3 + \eta) \frac{1}{r} \right) \mathbf{p}^2 - 2\eta (\hat{\mathbf{n}} \cdot \mathbf{p})^2 \frac{1}{r} + 2 \frac{\mathbf{S}_{\text{eff}} \cdot \mathbf{L}}{r^3} \quad . \end{aligned} \quad (\text{B20})$$

We can now re-write $\mathbf{a}_{2.5PN}$ of Eq. (A2) in terms of ADM variables as

$$\begin{aligned} \mathbf{a}_{2.5PN \rightarrow ADM} &= \frac{8}{5} \left(\frac{\eta}{r} \right) \times \{ \quad (\text{B21}) \\ &\frac{\hat{\mathbf{n}}}{r^2} \left[\dot{r} \left(\frac{17}{3r} + 3\mathbf{p}^2 + 3(3\eta - 1) \mathbf{p}^4 - 6(3 + \eta) \frac{\mathbf{p}^2}{r} - 6\eta \frac{(\hat{\mathbf{n}} \cdot \mathbf{p})^2}{r} + 6 \frac{\mathbf{S}_{\text{eff}} \cdot \mathbf{L}}{r^3} \right) + \eta (\hat{\mathbf{n}} \cdot \mathbf{p}) \left(\frac{3}{r^2} + \frac{\mathbf{p}^2}{r} \right) \right] \\ &- \frac{\mathbf{p}}{r^2} \left[\frac{3}{r} + \mathbf{p}^2 + \frac{3}{2} (3\eta - 1) \mathbf{p}^4 + \frac{1}{2} (3\eta - 21) \frac{\mathbf{p}^2}{r} - 3(3 + \eta) \frac{1}{r^2} - 2\eta \frac{(\hat{\mathbf{n}} \cdot \mathbf{p})^2}{r} + 2 \frac{\mathbf{S}_{\text{eff}} \cdot \mathbf{L}}{r^3} \right] \\ &- \frac{\mathbf{S}_{\text{eff}} \times \mathbf{r}}{r^5} \left(\frac{3}{r} + \mathbf{p}^2 \right) \} \quad . \end{aligned}$$

We can also replace \dot{r} with

$$\begin{aligned}\dot{r} &= \hat{\mathbf{n}} \cdot \mathbf{v} = \left(1 + \frac{1}{2}(3\eta - 1)\mathbf{p}^2 - (3 + \eta)\frac{1}{r}\right) \hat{\mathbf{n}} \cdot \mathbf{p} - \eta(\hat{\mathbf{n}} \cdot \mathbf{p})\frac{1}{r} \\ &= \left(1 + \frac{1}{2}(3\eta - 1)\mathbf{p}^2 - (3 + 2\eta)\frac{1}{r}\right) \hat{\mathbf{n}} \cdot \mathbf{p}\end{aligned}\tag{B22}$$

To get

$$\begin{aligned}\mathbf{a}_{2.5PN \rightarrow ADM} &= \frac{8}{5} \left(\frac{\eta}{r}\right) \times \{ \tag{B23} \\ &\frac{\hat{\mathbf{n}}}{r^2} \left[(\hat{\mathbf{n}} \cdot \mathbf{p}) \left(\frac{17}{3r} + 3\mathbf{p}^2 + \frac{9}{2}(3\eta - 1)\mathbf{p}^4 - \frac{1}{2} \left(5\eta + \frac{179}{3}\right) \frac{\mathbf{p}^2}{r} - \frac{1}{3} (25\eta + 51) \frac{1}{r^2} - 6\eta \frac{(\hat{\mathbf{n}} \cdot \mathbf{p})^2}{r} + 6 \frac{\mathbf{S}_{\text{eff}} \cdot \mathbf{L}}{r^3} \right) \right] \\ &- \frac{\mathbf{p}}{r^2} \left[\frac{3}{r} + \mathbf{p}^2 + \frac{3}{2}(3\eta - 1)\mathbf{p}^4 + \frac{1}{2}(3\eta - 21) \frac{\mathbf{p}^2}{r} - 3(3 + \eta) \frac{1}{r^2} - 2\eta \frac{(\hat{\mathbf{n}} \cdot \mathbf{p})^2}{r} + 2 \frac{\mathbf{S}_{\text{eff}} \cdot \mathbf{L}}{r^3} \right] \\ &- \frac{\mathbf{S}_{\text{eff}} \times \mathbf{r}}{r^5} \left(\frac{3}{r} + \mathbf{p}^2 \right) \} \quad .\end{aligned}$$

Since we used a coordinate change valid to 1PN order, Eqs. (B23 and B21) includes 3.5PN corrections as well as 2.5PN corrections.

To rewrite $\mathbf{a}_{3.5PN \rightarrow ADM}$ we simply take the harmonic expressions and replace $\mathbf{x} = \mathbf{r}$ and $\mathbf{v} = \mathbf{p}$, noting that $\tilde{\mathbf{L}}_N = \mathbf{L}$ to lowest order, and that the spins of Refs. [10, 11] are η times those of this section: $\mathcal{S}_i = \eta \mathbf{S}_i$.

Now, to incorporate the effects of dissipation, we can add the appropriately converted accelerations. Taking the time derivative of Eq. (B19) and rearranging to solve for $\dot{\mathbf{p}}$, there are additional corrections of the form

$$\dot{\mathbf{p}} = \dot{\mathbf{v}} \left(1 - \frac{1}{2}(3\eta - 1)\mathbf{p}^2 + (3 + \eta)\frac{1}{r} \right) - (3\eta - 1)(\mathbf{p} \cdot \dot{\mathbf{p}})\mathbf{p} + \eta(\hat{\mathbf{n}} \cdot \dot{\mathbf{p}})\frac{1}{r}\hat{\mathbf{n}} + \dots \tag{B24}$$

We then use $\dot{\mathbf{v}} = \mathbf{a}_{2.5PN \rightarrow ADM} + \mathbf{a}_{3.5PN \rightarrow ADM}$ and drop all terms higher than 3.5PN to get

$$\begin{aligned}\dot{\mathbf{p}} &= \dots + \mathbf{a}_{2.5PN \rightarrow ADM} \left(1 - \frac{1}{2}(3\eta - 1)\mathbf{p}^2 + (3 + \eta)\frac{1}{r} \right) + \mathbf{a}_{3.5PN \rightarrow ADM} + \\ &- (3\eta - 1)(\mathbf{p} \cdot \mathbf{a}_{2.5PN})\mathbf{p} + \eta(\hat{\mathbf{n}} \cdot \mathbf{a}_{2.5PN})\frac{1}{r}\hat{\mathbf{n}}\end{aligned}\tag{B25}$$

where we have only isolated the relevant half-order terms so “...” represents all the whole-order PN terms. Here $\mathbf{a}_{2.5PN \rightarrow ADM}$ is defined in Eq. (B23), and we replace $\dot{\mathbf{p}}$ where it occurs on the right hand side of (B25) with $\mathbf{a}_{2.5PN}$ evaluated at $\mathbf{x} = \mathbf{r}$, $\mathbf{v} = \mathbf{p}$. The term $\mathbf{a}_{3.5PN \rightarrow ADM}$ is also evaluated at $\mathbf{x} = \mathbf{r}$, $\mathbf{v} = \mathbf{p}$, and, again, the spins of the previous section

are related to these spins through $\mathcal{S}_i = \eta \mathbf{S}_i$, yielding

$$\begin{aligned} \tilde{\mathbf{a}}_{2.5PN \rightarrow ADM} &\equiv \mathbf{a}_{2.5PN \rightarrow ADM} \left(1 - \frac{1}{2} (3\eta - 1) \mathbf{p}^2 + (3 + \eta) \frac{1}{r} \right) = \\ &\frac{8}{5} \left(\frac{\eta}{r} \right) \times \left\{ \frac{\hat{\mathbf{n}}}{r^2} \left[\hat{\mathbf{n}} \cdot \mathbf{p} \left(\frac{17}{3r} + 3\mathbf{p}^2 + 3(3\eta - 1) \mathbf{p}^4 - 2(4\eta + 9) \frac{\mathbf{p}^2}{r} - \frac{8}{3} \frac{\eta}{r^2} - 6\eta \frac{(\hat{\mathbf{n}} \cdot \mathbf{p})^2}{r} + 6 \frac{\mathbf{S}_{\text{eff}} \cdot \mathbf{L}}{r^3} \right) \right] \right. \\ &\left. - \frac{\mathbf{p}}{r^2} \left[\frac{3}{r} + \mathbf{p}^2 + (3\eta - 1) \mathbf{p}^4 - 2(\eta + 3) \frac{\mathbf{p}^2}{r} - 2\eta \frac{(\hat{\mathbf{n}} \cdot \mathbf{p})^2}{r} + 2 \frac{\mathbf{S}_{\text{eff}} \cdot \mathbf{L}}{r^3} \right] \right. \\ &\left. - \frac{\mathbf{S}_{\text{eff}} \times \mathbf{r}}{r^5} \left(\frac{3}{r} + \mathbf{p}^2 \right) \right\} \quad , \end{aligned} \quad (\text{B26})$$

Finally, our equations of motion become

$$\begin{aligned} \dot{\mathbf{r}} &= A\mathbf{p} + B\hat{\mathbf{n}} + \frac{\mathbf{S}_{\text{eff}} \times \mathbf{r}}{r^3} \\ \dot{\mathbf{p}} &= C\mathbf{p} + D\hat{\mathbf{n}} + \frac{\mathbf{S}_{\text{eff}} \times \mathbf{p}}{r^3} + \frac{3\hat{\mathbf{n}}}{r} H_{SO} - \frac{\partial H_{SS}}{\partial \mathbf{r}} + \tilde{\mathbf{a}}_{2.5PN \rightarrow ADM} + \mathbf{a}_{3.5PN \rightarrow ADM} \\ &\quad + \eta(\hat{\mathbf{n}} \cdot \mathbf{a}_{2.5PN}) \frac{1}{r} \hat{\mathbf{n}} - (3\eta - 1)(\mathbf{p} \cdot \mathbf{a}_{2.5PN}) \mathbf{p} \end{aligned} \quad (\text{B27})$$

We can regroup the accelerations to 2.5 order and 3.5 orders in ADM variables:

$$\begin{aligned} \dot{\mathbf{r}} &= A\mathbf{p} + B\hat{\mathbf{n}} + \frac{\mathbf{S}_{\text{eff}} \times \mathbf{r}}{r^3} \\ \dot{\mathbf{p}} &= C\mathbf{p} + D\hat{\mathbf{n}} + \frac{\mathbf{S}_{\text{eff}} \times \mathbf{p}}{r^3} + \frac{3\hat{\mathbf{n}}}{r} H_{SO} - \frac{\partial H_{SS}}{\partial \mathbf{r}} + \mathbf{a}_{ADM}^{(2.5)} + \mathbf{a}_{ADM}^{(3.5)} \end{aligned} \quad (\text{B28})$$

with

$$\mathbf{a}_{ADM}^{(2.5)} = \frac{8}{5} \left(\frac{\eta}{r} \right) \times \left\{ \frac{\hat{\mathbf{n}}}{r^2} \left[\hat{\mathbf{n}} \cdot \mathbf{p} \left(\frac{17}{3r} + 3\mathbf{p}^2 \right) \right] - \frac{\mathbf{p}}{r^2} \left[\frac{3}{r} + \mathbf{p}^2 \right] \right\} \quad , \quad (\text{B29})$$

and using

$$\begin{aligned} \eta(\hat{\mathbf{n}} \cdot \mathbf{a}_{2.5PN}) \frac{1}{r} \hat{\mathbf{n}} &= \left(\frac{8\eta}{5r} \right) \frac{\hat{\mathbf{n}}}{r^2} (\hat{\mathbf{n}} \cdot \mathbf{p}) \left(\frac{8\eta}{3r^2} + 2\eta \frac{\mathbf{p}^2}{r} \right) \\ -(3\eta - 1)(\mathbf{p} \cdot \mathbf{a}_{2.5PN}) \mathbf{p} &= \left(\frac{8\eta}{5r} \right) \left(-\frac{\mathbf{p}}{r^2} \right) (3\eta - 1) \left[(\hat{\mathbf{n}} \cdot \mathbf{p})^2 \left(\frac{17}{3r} + 3\mathbf{p}^2 \right) - \mathbf{p}^2 \left(\frac{3}{r} + \mathbf{p}^2 \right) \right] \end{aligned} \quad (\text{B30})$$

and the 3.5PN piece in $\tilde{\mathbf{a}}_{2.5PN \rightarrow ADM}$

$$\begin{aligned} \dots \frac{8}{5} \left(\frac{\eta}{r} \right) \times \left\{ \frac{\hat{\mathbf{n}}}{r^2} \left[\hat{\mathbf{n}} \cdot \mathbf{p} \left(3(3\eta - 1) \mathbf{p}^4 - 2(4\eta + 9) \frac{\mathbf{p}^2}{r} - \frac{8}{3} \frac{\eta}{r^2} - 6\eta \frac{(\hat{\mathbf{n}} \cdot \mathbf{p})^2}{r} + 6 \frac{\mathbf{S}_{\text{eff}} \cdot \mathbf{L}}{r^3} \right) \right] \right. \\ \left. - \frac{\mathbf{p}}{r^2} \left[(3\eta - 1) \mathbf{p}^4 - 2(\eta + 3) \frac{\mathbf{p}^2}{r} - 2\eta \frac{(\hat{\mathbf{n}} \cdot \mathbf{p})^2}{r} + 2 \frac{\mathbf{S}_{\text{eff}} \cdot \mathbf{L}}{r^3} \right] \right. \\ \left. - \frac{\mathbf{S}_{\text{eff}} \times \mathbf{r}}{r^5} \left(\frac{3}{r} + \mathbf{p}^2 \right) \right\} \quad , \end{aligned} \quad (\text{B31})$$

and adding all of these 3.5PN pieces to

$$\begin{aligned} \mathbf{a}_{3.5PN \rightarrow ADM} = & \frac{8}{5}\eta \left(\frac{1}{r}\right) \times \{ \\ & -\frac{\hat{\mathbf{n}}}{r^2}(\hat{\mathbf{n}} \cdot \mathbf{p}) \left[\frac{23}{14}(43 + 14\eta) \left(\frac{1}{r}\right)^2 + \frac{3}{28}(61 + 70\eta)\mathbf{p}^4 + 70(\hat{\mathbf{n}} \cdot \mathbf{p})^4 \right. \\ & + \frac{1}{42}(519 - 1267\eta) \left(\frac{1}{r}\right) \mathbf{p}^2 + \frac{1}{4}(147 + 188\eta) \left(\frac{1}{r}\right) (\hat{\mathbf{n}} \cdot \mathbf{p})^2 - \frac{15}{4}(19 + 2\eta) \mathbf{p}^2(\hat{\mathbf{n}} \cdot \mathbf{p})^2 \left. \right] \\ & + \frac{\mathbf{p}}{r^2} \left[\frac{1}{42}(1325 + 546\eta) \left(\frac{1}{r}\right)^2 + \frac{1}{28}(313 + 42\eta) \mathbf{p}^4 + 75(\hat{\mathbf{n}} \cdot \mathbf{p})^4 \right. \\ & \left. - \frac{1}{42}(205 + 777\eta) \left(\frac{1}{r}\right) \mathbf{p}^2 + \frac{1}{12}(205 + 424\eta) \left(\frac{1}{r}\right) \dot{r}^2 - \frac{3}{4}(113 + 2\eta) \mathbf{p}^2(\hat{\mathbf{n}} \cdot \mathbf{p})^2 \right] \} . \end{aligned}$$

gives

$$\begin{aligned} \mathbf{a}_{ADM}^{(3.5)} = & \frac{8}{5}\eta \left(\frac{1}{r}\right) \times \{ \\ & -\frac{\hat{\mathbf{n}}}{r^2}(\hat{\mathbf{n}} \cdot \mathbf{p}) \left[\frac{1}{14}(989 + 322\eta) \left(\frac{1}{r}\right)^2 + \frac{3}{28}(89 - 14\eta) \mathbf{p}^4 + 70(\hat{\mathbf{n}} \cdot \mathbf{p})^4 \right. \\ & + \frac{1}{42}(1275 - 1015\eta) \left(\frac{1}{r}\right) \mathbf{p}^2 + \frac{1}{4}(147 + 212\eta) \left(\frac{1}{r}\right) (\hat{\mathbf{n}} \cdot \mathbf{p})^2 - \frac{15}{4}(19 + 2\eta) \mathbf{p}^2(\hat{\mathbf{n}} \cdot \mathbf{p})^2 - 6\frac{\mathbf{S}_{\text{eff}} \cdot \mathbf{L}}{r^3} \left. \right] \\ & + \frac{\mathbf{p}}{r^2} \left[\frac{1}{42}(1325 + 546\eta) \left(\frac{1}{r}\right)^2 + \frac{1}{28}(313 + 42\eta) \mathbf{p}^4 + 75(\hat{\mathbf{n}} \cdot \mathbf{p})^4 + \frac{1}{12}(273 + 244\eta) \frac{(\hat{\mathbf{n}} \cdot \mathbf{p})^2}{r} \right. \\ & \left. - \frac{1}{42}(79 + 315\eta) \left(\frac{1}{r}\right) \mathbf{p}^2 - \frac{1}{4}(327 + 42\eta) \mathbf{p}^2(\hat{\mathbf{n}} \cdot \mathbf{p})^2 - 2\frac{\mathbf{S}_{\text{eff}} \cdot \mathbf{L}}{r^3} \right] \\ & \left. - \frac{\mathbf{S}_{\text{eff}} \times \mathbf{r}}{r^5} \left(\frac{3}{r} + \mathbf{p}^2\right) \right\} . \end{aligned}$$

Then there are the spin pieces:

$$\begin{aligned} \mathbf{a}_{ADM}^{(3.5PN-SO)} = & -\frac{\eta^2}{5r^4} \left\{ \frac{(\hat{\mathbf{n}} \cdot \mathbf{p})\hat{\mathbf{n}}}{r} \left[\left(120\mathbf{p}^2 + 280(\hat{\mathbf{n}} \cdot \mathbf{p})^2 + 453\frac{1}{r}\right) \mathbf{L} \cdot \mathbf{S} \right. \right. \\ & + \left. \left(120\mathbf{p}^2 + 280(\hat{\mathbf{n}} \cdot \mathbf{p})^2 + 458\frac{1}{r}\right) \mathbf{L} \cdot \xi_{ADM} \right] \\ & + \frac{\mathbf{p}}{r} \left[\left(87\mathbf{p}^2 - 675(\hat{\mathbf{n}} \cdot \mathbf{p})^2 - \frac{901}{3}\frac{1}{r}\right) \mathbf{L} \cdot \mathbf{S} + 4 \left(18\mathbf{p}^2 - 150(\hat{\mathbf{n}} \cdot \mathbf{p})^2 - 66\frac{1}{r}\right) \mathbf{L} \cdot \xi_{ADM} \right] \\ & - \frac{2}{3}(\hat{\mathbf{n}} \cdot \mathbf{p})\mathbf{p} \times \mathbf{S} \left(48\mathbf{p}^2 + 15(\hat{\mathbf{n}} \cdot \mathbf{p})^2 + 364\frac{1}{r}\right) + \frac{1}{3}(\hat{\mathbf{n}} \cdot \mathbf{p})\mathbf{p} \times \xi_{ADM} \left(291\mathbf{p}^2 - 705(\hat{\mathbf{n}} \cdot \mathbf{p})^2 - 772\frac{1}{r}\right) \\ & + \frac{1}{2}\hat{\mathbf{n}} \times \mathbf{S} \left(31\mathbf{p}^4 - 260\mathbf{p}^2(\hat{\mathbf{n}} \cdot \mathbf{p})^2 + 245(\hat{\mathbf{n}} \cdot \mathbf{p})^4 - \frac{689}{3}\mathbf{p}^2\frac{1}{r} + 537(\hat{\mathbf{n}} \cdot \mathbf{p})^2\frac{1}{r} + \frac{4}{3}\frac{1}{r^2}\right) \\ & \left. + \frac{1}{2}\hat{\mathbf{n}} \times \xi_{ADM} \left(115\mathbf{p}^4 - 1130\mathbf{p}^2(\hat{\mathbf{n}} \cdot \mathbf{p})^2 + 1295(\hat{\mathbf{n}} \cdot \mathbf{p})^4 - \frac{869}{3}\mathbf{p}^2\frac{1}{r} + 849(\hat{\mathbf{n}} \cdot \mathbf{p})^2\frac{1}{r} + \frac{44}{3}\frac{1}{r^2}\right) \right\} . \end{aligned} \tag{B32}$$

and

$$\begin{aligned}
\mathbf{a}_{ADM}^{(3.5PN-SS)} = & \frac{\eta^2}{r^5} \left\{ \hat{\mathbf{n}} \left[\left(287(\hat{\mathbf{n}} \cdot \mathbf{p})^2 - 99\mathbf{p}^2 + \frac{541}{5} \frac{1}{r} \right) (\hat{\mathbf{n}} \cdot \mathbf{p})(\mathbf{S}_1 \cdot \mathbf{S}_2) \right. \right. \\
& - \left(2646(\hat{\mathbf{n}} \cdot \mathbf{p})^2 - 714\mathbf{p}^2 + \frac{1961}{5} \frac{1}{r} \right) (\hat{\mathbf{n}} \cdot \mathbf{p})(\hat{\mathbf{n}} \cdot \mathbf{S}_1)(\hat{\mathbf{n}} \cdot \mathbf{S}_2) \\
& + \left. \left(1029(\hat{\mathbf{n}} \cdot \mathbf{p})^2 - 123\mathbf{p}^2 + \frac{629}{10} \frac{1}{r} \right) ((\hat{\mathbf{n}} \cdot \mathbf{S}_1)(\mathbf{p} \cdot \mathbf{S}_2) + (\hat{\mathbf{n}} \cdot \mathbf{S}_2)(\mathbf{p} \cdot \mathbf{S}_1)) - 336(\hat{\mathbf{n}} \cdot \mathbf{p})(\mathbf{p} \cdot \mathbf{S}_1)(\mathbf{p} \cdot \mathbf{S}_2) \right] \\
& + \mathbf{p} \left[\left(\frac{171}{5} \mathbf{p}^2 - 195(\hat{\mathbf{n}} \cdot \mathbf{p})^2 - 67 \frac{1}{r} \right) (\mathbf{S}_1 \cdot \mathbf{S}_2) - \left(174\mathbf{p}^2 - 1386(\hat{\mathbf{n}} \cdot \mathbf{p})^2 - \frac{1038}{5} \frac{1}{r} \right) (\hat{\mathbf{n}} \cdot \mathbf{S}_1)(\hat{\mathbf{n}} \cdot \mathbf{S}_2) \right. \\
& - 438(\hat{\mathbf{n}} \cdot \mathbf{p}) ((\hat{\mathbf{n}} \cdot \mathbf{S}_1)(\mathbf{p} \cdot \mathbf{S}_2) + (\hat{\mathbf{n}} \cdot \mathbf{S}_2)(\mathbf{p} \cdot \mathbf{S}_1)) + 96(\mathbf{p} \cdot \mathbf{S}_1)(\mathbf{p} \cdot \mathbf{S}_2) \\
& + \left(\frac{27}{10} \mathbf{p}^2 - \frac{75}{2} (\hat{\mathbf{n}} \cdot \mathbf{p})^2 - \frac{509}{30} \frac{1}{r} \right) ((\mathbf{p} \cdot \mathbf{S}_2)\mathbf{S}_1 + (\mathbf{p} \cdot \mathbf{S}_1)\mathbf{S}_2) \\
& \left. + \left(\frac{15}{2} \mathbf{p}^2 + \frac{77}{2} (\hat{\mathbf{n}} \cdot \mathbf{p})^2 + \frac{199}{10} \frac{1}{r} \right) (\hat{\mathbf{n}} \cdot \mathbf{p}) ((\hat{\mathbf{n}} \cdot \mathbf{S}_2)\mathbf{S}_1 + (\hat{\mathbf{n}} \cdot \mathbf{S}_1)\mathbf{S}_2) \right\} . \tag{B33}
\end{aligned}$$

with $\xi_{ADM} \equiv (m_2/m_1)\mathbf{S}_1 + (m_1/m_2)\mathbf{S}_2$.

Given the equations of this section and the previous section, the equations of motion can be evolved in either set of variables.

In §II we introduced the (r, Φ, Ψ) coordinates. The equations of motion (B28) can be projected onto this basis as was done in Refs. [19, 20].

-
- [1] G. Schafer, *Annals Phys.* **161**, 81 (1985).
 - [2] T. Damour and N. Deruelle, *C. R. Acad. Sci. Paris* **293**, 537 (1981).
 - [3] T. Damour and G. Schafer, *Nuovo Cim.* **B101**, 127 (1988).
 - [4] P. Jaranowski and G. Schafer, *erratum-ibid.d* **63**, 029902 (2001).
 - [5] T. Damour, P. Jaranowski, and G. Schafer, *Phys. Lett. B* **513**, 147 (2001).
 - [6] T. Damour, P. Jaranowski, and G. Schafer, *Phys. Rev. D* **62**, 084011 (2000).
 - [7] B. R. Iyer and C. M. Will, *Phys. Rev. D* **52**, 6882 (1995).
 - [8] T. Mora and C. M. Will, *Phys. Rev.* **D69**, 104021 (2004).
 - [9] M. E. Pati and C. M. Will, *Phys. Rev.* **D65**, 104008 (2002).
 - [10] C. M. Will, *Phys. Rev.* **D71**, 084027 (2005).
 - [11] H. Wang and C. M. Will, *Phys. Rev.* **D75**, 064017 (2007).
 - [12] A. Sesana, *Astrophys. J.* **719**, 851 (2010).
 - [13] L. Wen, *Ap. J.* **598**, 419 (2003).

- [14] R. M. O’Leary, B. Kocsis, and A. Loeb, (2008).
- [15] K. Glampedakis, *Class. Quant. Grav.* **22**, S605 (2005).
- [16] J. Levin and G. Perez-Giz, *Phys. Rev.* **D77**, 103005 (2008).
- [17] F. Pretorius and D. Khurana, *Class. Quant. Grav.* **24**, S83 (2007).
- [18] J. Healy, J. Levin, and D. Shoemaker, *Phys. Rev. Lett.* **103**, 131101 (2009).
- [19] J. Levin and B. Grossman, *Phys. Rev.* **D79**, 043016 (2009).
- [20] R. Grossman and J. Levin, *Phys. Rev.* **D79**, 043017 (2009).
- [21] L. E. Kidder, C. M. Will, and A. G. Wiseman, *Phys. Rev. D* **47**, 4183 (1993).
- [22] L. E. Kidder, *Phys. Rev. D* **52**, 821 (1995).
- [23] A. Buonanno, Y. Chen, and T. Damour, *Phys. Rev.* **D74**, 104005 (2006).
- [24] 2011, private communication.
- [25] N. Yunes and E. Berti, *Phys. Rev. D* **77**, 124006 (2008).
- [26] K. G. Arun, A. Buonanno, G. Faye, and E. Ochsner, *Phys. Rev. D* **79**, 104023 (2009).
- [27] G. Faye, L. Blanchet, and A. Buonanno, *Phys. Rev. D* **74**, 104033 (2006).